AD-A131 372 BIOLOGICAL EFFECTS OF MILLIMETER-WAVE IRRADIATION(U) 1/1
UTAH UNIV SALT LAKE CITY DEPT OF ELECTRICAL ENGINEERING
O P GANDHI ET AL. DEC 82 UTEC-82-075 SAM-TR-82-49
UNCLASSIFIED F33615-81-K-0613 F/G 6/18 NL

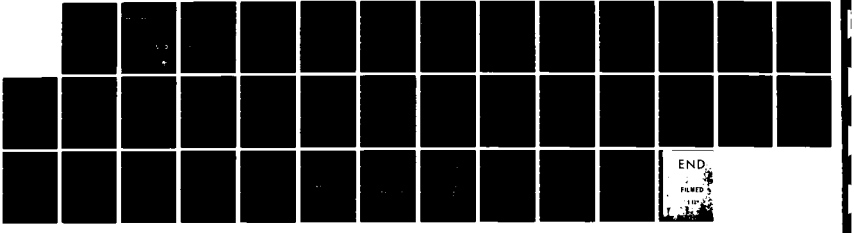

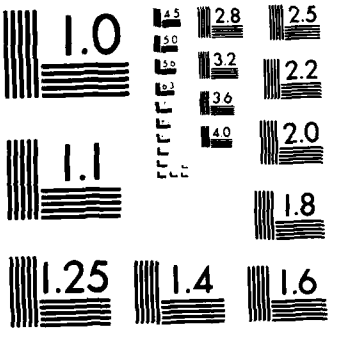

Report USAFSAM-TR-82-49

(12)

BIOLOGICAL EFFECTS OF MILLIMETER-WAVE IRRADIATION

O. P. Gandhi, Sc.D.
D. W. Hill, Ph.D.
A. Riazi, Ph.D.
P. Wahid, Ph.D.
C. H. Wang, Ph.D.
M. F. Iskander, Ph.D.

Department of Electrical Engineering
University of Utah
Salt Lake City, Utah 84112

December 1982

Final Report for Period 15 May 1981 - 30 June 1982

Prepared for
USAF SCHOOL OF AEROSPACE MEDICINE
Aerospace Medical Division (AFSC)
Brooks Air Force Base, Texas 78235

NOTICES

This final report was submitted by the Department of Electrical Engineering, University of Utah, Salt Lake City, Utah 84112, under contract F33615-81-K-0613, job order 2312-V7-11, with the USAF School of Aerospace Medicine, Aerospace Medical Division, AFSC, Brooks Air Force Base, Texas. Dr. David N. Erwin (USAFSAM/RZP) was the Laboratory Project Scientist-in-Charge.

When Government drawings, specifications, or other data are used for any purpose other than in connection with a definitely Government-related procurement, the United States Government incurs no responsibility or any obligation whatsoever. The fact that the Government may have formulated or in any way supplied the said drawings, specifications, or other data, is not to be regarded by implication, or otherwise in any manner construed, as licensing the holder, or any other person or corporation; or as conveying any rights or permission to manufacture, use, or sell any patented invention that may in any way be related thereto.

The Office of Public Affairs has reviewed this report, and it is releasable to the National Technical Information Service, where it will be available to the general public, including foreign nationals.

This report has been reviewed and is approved for publication.

David N Erwin

DAVID N. ERWIN, Ph.D.
Project Scientist

John C Mitchell

JOHN C. MITCHELL, B.S.
Supervisor

Roy L DeHart

ROY L. DEHART
Colonel, USAF, MC
Commander

UNCLASSIFIED

SECURITY CLASSIFICATION OF THIS PAGE (When Data Entered)

REPORT DOCUMENTATION PAGE	READ INSTRUCTIONS BEFORE COMPLETING FORM
1. REPORT NUMBER: SAM-TR-82-49	2. GOVT ACCESSION NO.: AD-A131372
	3. RECIPIENT'S CATALOG NUMBER:
4. TITLE (and Subtitle): BIOLOGICAL EFFECTS OF MILLIMETER-WAVE IRRADIATION	5. TYPE OF REPORT & PERIOD COVERED: Final Report 15 May 1981-30 June 1982
	6. PERFORMING ORG. REPORT NUMBER: UTEC-82-075
7. AUTHOR(s): O. P. Gandhi, Sc.D.; D. W. Hill, Ph.D.; A. Riazi, Ph.D.; P. Wahid, Ph.D.; C. H. Wang, Ph.D.; and M. F. Iskander, Ph.D.	8. CONTRACT OR GRANT NUMBER(s): F33615-81-K-0613
9. PERFORMING ORGANIZATION NAME AND ADDRESS: Department of Electrical Engineering, University of Utah, Salt Lake City, Utah 84112	10. PROGRAM ELEMENT, PROJECT, TASK AREA & WORK UNIT NUMBERS: 61102F, 2312-V7-11
11. CONTROLLING OFFICE NAME AND ADDRESS: USAF School of Aerospace Medicine (RZP), Aerospace Medical Division (AFSC), Brooks AFB, Texas 78235	12. REPORT DATE: December 1982
	13. NUMBER OF PAGES: 33
14. MONITORING AGENCY NAME & ADDRESS (if different from Controlling Office)	15. SECURITY CLASS. (of this report): Unclassified
	15a. DECLASSIFICATION/DOWNGRADING SCHEDULE

16. DISTRIBUTION STATEMENT (of this Report)

Approved for public release; distribution unlimited.

17. DISTRIBUTION STATEMENT (of the abstract entered in Block 20, if different from Report)

18. SUPPLEMENTARY NOTES

19. KEY WORDS (Continue on reverse side if necessary and identify by block number)

Millimeter waves	Broadband dosimetrically quantifiable irradiation system
Mutagenic effects	Brillouin and Raman spectroscopy of biological media
Escherichia coli	Salmonella typhimurium
Infinite sample method	Complex permittivities

20 ABSTRACT (Continue on reverse side if necessary and identify by block number)

The report describes experiments on millimeter-wave effects on lambda-prophage induction in lysogenic strains of E. coli, temperature-sensitive mutants of lambda prophage, and Salmonella typhimurium cells possessing His mutation. No frequency-sensitive irradiation effects have been observed in spite of closely spaced frequencies used in the 42-48 and 65-75 GHz bands. A new method for measuring complex permittivities of biological media, with potential for in-vivo measurements, has been proposed that alleviates the need for samples with submillimeter thicknesses. Initial results (continued)

DD FORM 1 JAN 73 1473 EDITION OF 1 NOV 65 IS OBSOLETE

UNCLASSIFIED

SECURITY CLASSIFICATION OF THIS PAGE (When Data Entered)

20. ABSTRACT (continued)
appear to be highly promising. A system to allow low-wave-number Raman and Brillouin spectroscopy of biological media has also been set up.

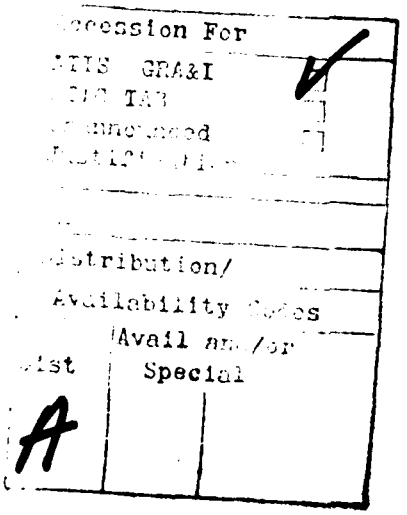

BIOLOGICAL EFFECTS OF MILLIMETER-WAVE IRRADIATION

INTRODUCTION

With the recent advances in millimeter-wave technology, including the availability of high-power transmitters in this band, the interaction of fields at these frequencies with biological media must be understood. Several research reports [1-4] indicate sharp millimeter-wave frequency-dependent lethal and mutagenic effects on microorganisms, and major effects on metabolic control of cell growth. A basic knowledge of the dielectric properties of biological media is needed to judge the validity of these claims or to guess about the frequency regions of greatest interest. To search for frequency-specific effects, evaluation of the action spectra of millimeter-wave irradiation is inefficient, relying as it does on fairly time-consuming biological and biochemical assays. One such study undertaken by us for protein synthesis by baby hamster kidney (BHK) mammalian cells [5-7] with and without CW irradiation, for 200 frequencies at 0.1-GHz intervals in the 38- to 48-GHz and 65- to 75-GHz bands, failed to reveal any microwave-induced effects as compared to control samples. Other studies are currently underway in our laboratory to examine the change in mutation rates of bacteria and their specific viruses.

With conventional approaches, accurate measurements of the complex permittivities of the biological media have been difficult at millimeter wavelengths requiring precisely fabricated sample holders [8, 9] covering fairly narrow bandwidths. Also, because of very high attenuation constants on the order of 150-300 dB/cm, the thickness of the conventional sample holders has had to be a fraction of a millimeter, with concomitant problems of air bubbles and nonuniform filling densities for biological tissues. We are evaluating a new and novel approach that may alleviate these problems, making it possible to obtain the absolute permittivities of biological tissues over the 26.5- to 90-GHz band for which the solid-state computer-controlled precision measurement facilities [10] are currently available in our laboratory. Knowledge of complex permittivities

of biological preparations and tissues is needed for dosimetry and is valuable in anticipating any frequency-specific effects.

Determining the mechanisms of interaction between electromagnetic fields and biological media is an important aspect of research in the RFR-bioeffects area. A promising line of investigation suggested toward this objective is the laser Brillouin and Raman spectral studies of the biological media. Laser Brillouin spectroscopy [11, 12] has the advantage of being able to emit (launch) or absorb acoustic phonons in a medium at frequencies on the order of 0.1-1.0 cm^{-1} (3-30 GHz). For higher frequency optical phonons ($\geq$ 5-10 cm^{-1}), Raman spectroscopy is more appropriate. The dimensions of the biological membranes and molecules are on the order of tens of angstroms to several thousand angstroms and comparable to the wavelength of acoustic waves at microwave/millimeter frequencies in these media. It is entirely conceivable, therefore, that Brillouin and Raman spectral studies will provide a new and useful means of studying these media, particularly the mechanisms of interaction at microwave frequencies. Fröhlich [13] has alluded to the possibility that specific frequencies of a biological system are related to the excitability of acoustic phonons in cells. We propose using Raman spectroscopy as a physical tool for evaluating frequency-specific effects of millimeter-wave irradiation. The bioassays used by us [5-7] and others to search for frequency-specific effects are fairly time consuming. Another disadvantage is that bioeffects during irradiation, if any, are not detected because of the technique's lack of spontaneity.

MUTAGENIC EFFECTS OF MILLIMETER-WAVE IRRADIATION

Effects on Wild-type Lambda Phage Induction

The dosimetrically quantifiable, temperature-compensated, broadband exposure system [14] developed on this project was used to study the reported effects of millimeter waves upon living bacterial organisms. Because of the ease of lambda-phage induction in lysogenic strains of Escherichia coli and the vast amount of supporting biochemical and genetic

information relative to the molecular mechanisms of action, this system was selected for the first study.

Strains of wild-type lambda phage and E. coli (TC600) were obtained from Dr. Costa Georgopoulos. Many isolates of lysogens were prepared and characterized with respect to effects of temperature, mitomycin C, and ultraviolet light on frequency of induction. The lysogen chosen (y-3) for use showed sensitivity to induction by mitomycin C and ultraviolet light, but typical wild-type insensitivity to induction at temperatures as high as 39°C.

The experimental design and the conditions of the experiments were as follows. Eighteen-hour log-phase cultures of the test lysogen were prepared; the organisms were harvested by centrifugation and resuspended in fresh growth medium. Immediately prior to use, the organisms were diluted to appropriate cell concentrations. The circulating exposure systems were then inoculated with measured volumes of these suspensions. After careful temperature equilibration of both control and experimental test suspensions, they were exposed to microwave irradiation at fixed powers and at the frequencies indicated in Figure 1 in both the U- and E-bands. The temperature differentials of the output ports of the test and control cells were continuously measured and recorded during the 30 minutes of exposure. The two cell suspensions were removed from the exposure systems, quantitatively diluted, and assayed for lambda phage by the appropriate indicator strain of E. coli. After overnight incubation at 37°C, the plaques were counted and the resulting data converted arithmetically into differences in frequency of induction of irradiated cells and control cells maintained at isothermal conditions.

The data collected from numerous individual experiments are summarized graphically in Figure 1. The data are plotted as differences in percentage of induction of irradiated and nonirradiated (control) cells versus frequencies in both the U- and E-bands. The mean values and the standard derivation (SD) for the difference $F_I - F_C$ in induction rates of wild-type phage are shown in Figures 2 and 3 for U- and E-bands respectively.

In all experiments undertaken so far, no significant effects have been observed at the indicated frequencies or power levels. It is to be

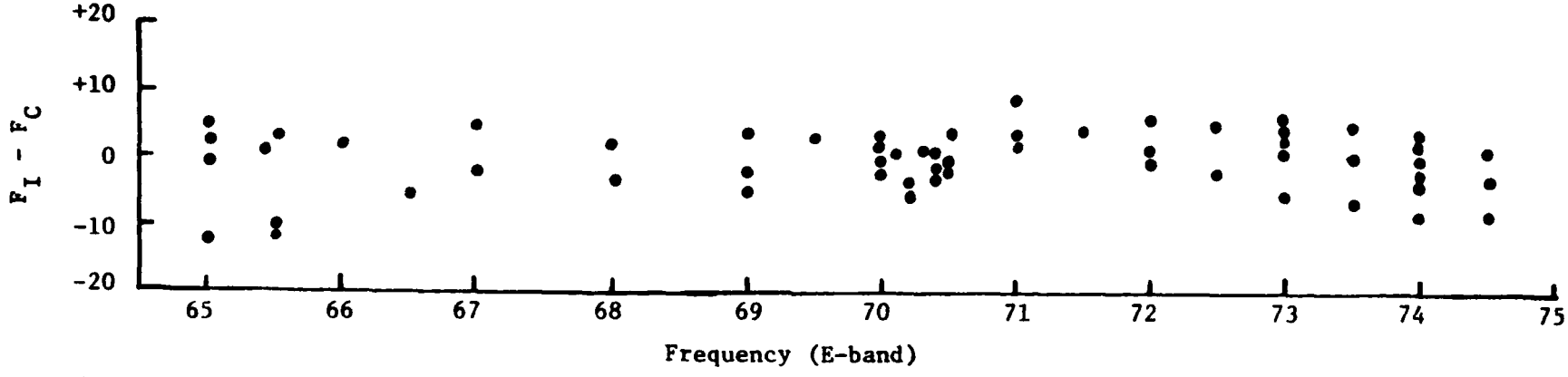

(a)

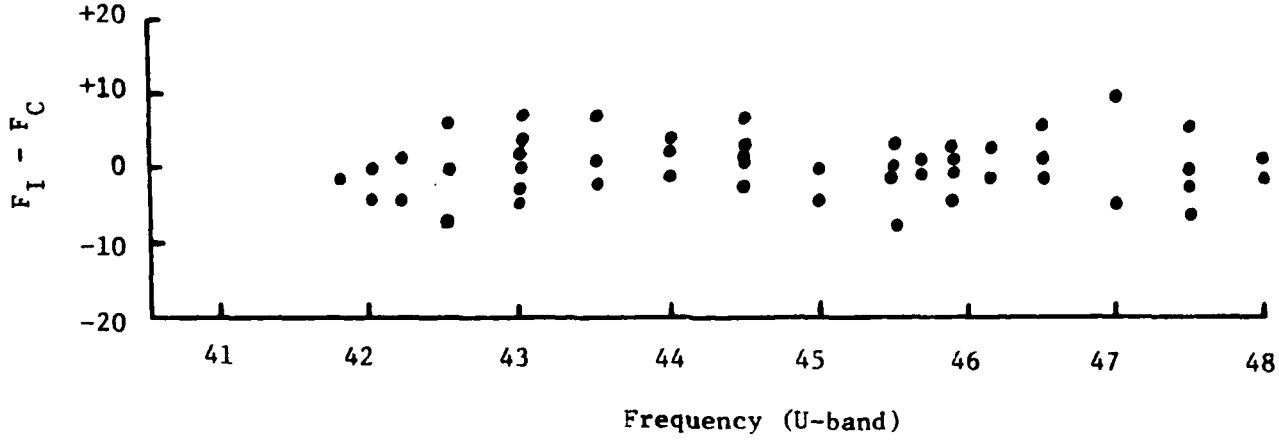

(b)

Figure 1. Effects of microwave irradiation on induction of lambda phage. ($F_I - F_C$ denotes the difference in percentage of induction between irradiated and control samples.)

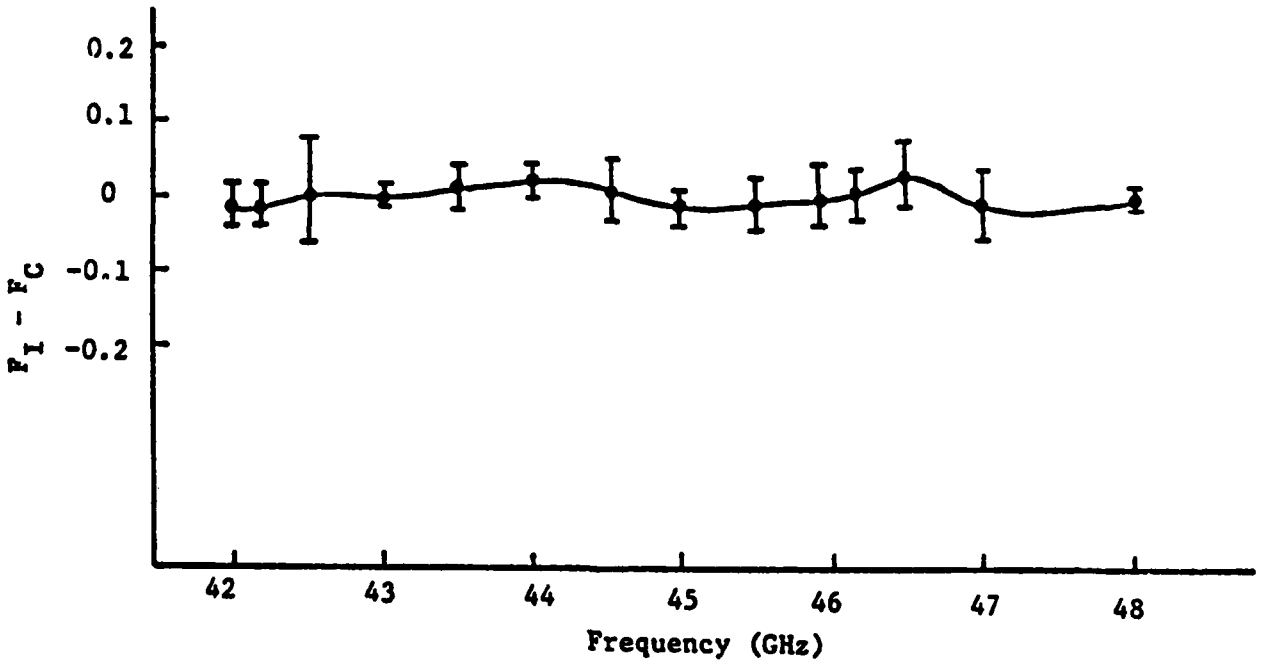

Figure 2. Effects of microwave irradiation on induction of lambda phage TC600 (λ papa). $F_I - F_C$ denotes the difference in induction rate between irradiated and control samples.

emphasized that these data were collected under very carefully controlled temperature conditions, both measurement and continuous recording. At no time during the 30-minute exposure were temperature differences at the exit ports allowed to exceed ±0.02°C. Thus at the same temperatures, control (nonirradiated) and irradiated cells of lysogenic E. coli exhibited no differences in frequencies of induction when exposed to millimeter microwaves.

Effects on Temperature-sensitive Mutants of Lambda Phage

The same experimental designs and procedures were subsequently used with temperature-sensitive mutants of lambda phage. These mutants show

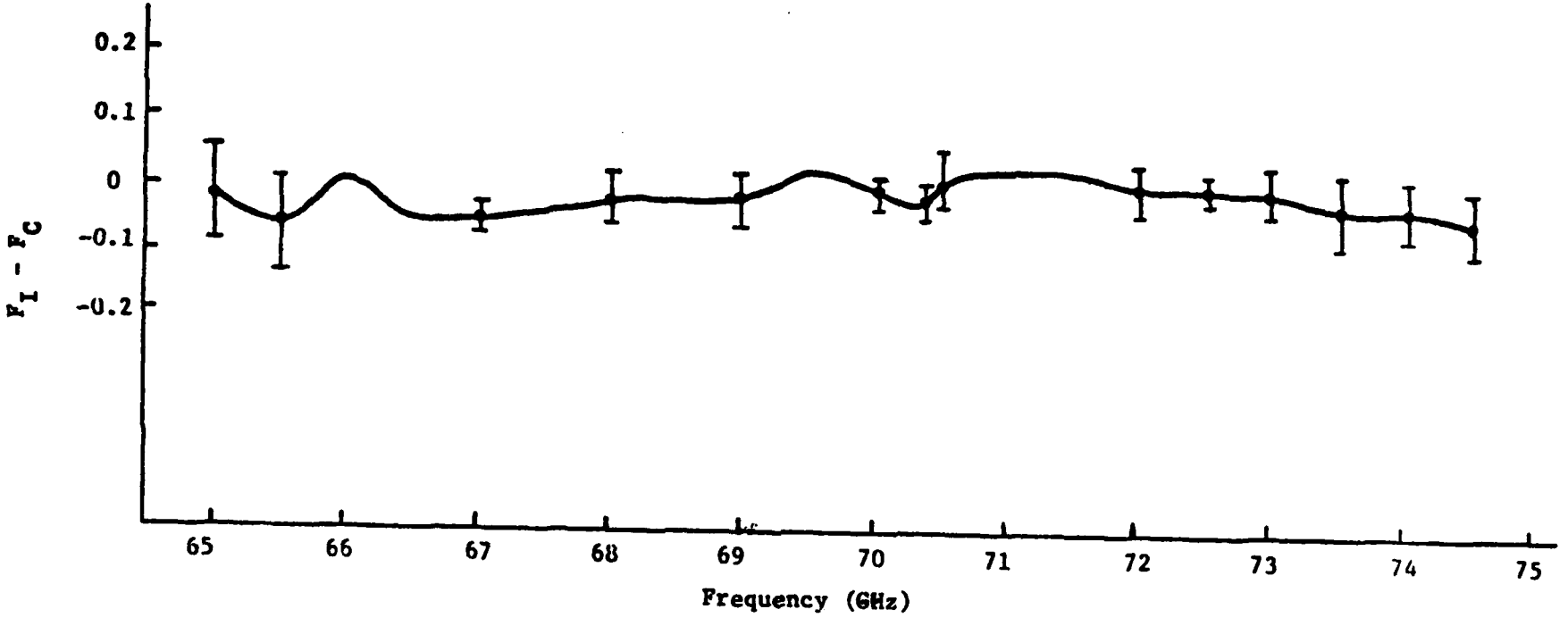

Figure 3. The difference in induction ($F_I - F_C$) for irradiated and control cells as a function of irradiation frequency (in the E-band) using lambda phage TC600 (λ papa).

characteristics of extreme sensitivity to heat induction. Several isolates of temperature-sensitive mutants of lambda phage C600 were obtained from Dr. Margaret Leib at the University of Southern California. They were purified, characterized, and tested regarding thermal sensitivity of induction and response to ultraviolet irradiation. Microwave experiments were then carried out for irradiation frequencies between 65 and 75 GHz, and 42 and 48 GHz. A frequency increment of 0.5 GHz was generally used; however, in the important frequency range of 70.1-70.5 GHz (where significant bioeffects have been reported [15]), a frequency increment of 0.1 GHz was used. During each 30-minute exposure, the temperature difference between the control and the irradiated samples was constantly monitored; electric heating of control samples was used to compensate for microwave heating of irradiated samples. The difference in fractional induction of lambda phage C600 (U16) between irradiated and control samples is shown in Figure 4 as a function of frequency. Our experiments indicate no significant differences between the induction rates of irradiated and control cells, even for these highly temperature-sensitive preparations.

Effects on Back-Mutation of His^- Salmonella typhimurium

Irradiation experiments have also been performed on Salmonella typhimurium cells (strain type TA1535) possessing His^- mutation (due to a base-pair mutation). The microwave power was 14 mW for E-band, 10 mW for U-band; and the frequency increment was 0.5 GHz. The mean values and the SD for the number of revertant colonies are shown in Figures 5 and 6 for U- and E-bands respectively. Once again, we have not observed a significant difference in back mutation between control and irradiated samples.

Two papers are being prepared to report the results of the above experiments.

Effects on Yeast Cell Growth Rate

Highly frequency-specific growth rates of yeast cells have been reported by Grundler and Keilmann [16] and Grundler [4] of Max Planck Institute in Stuttgart, West Germany, when they used millimeter-wave

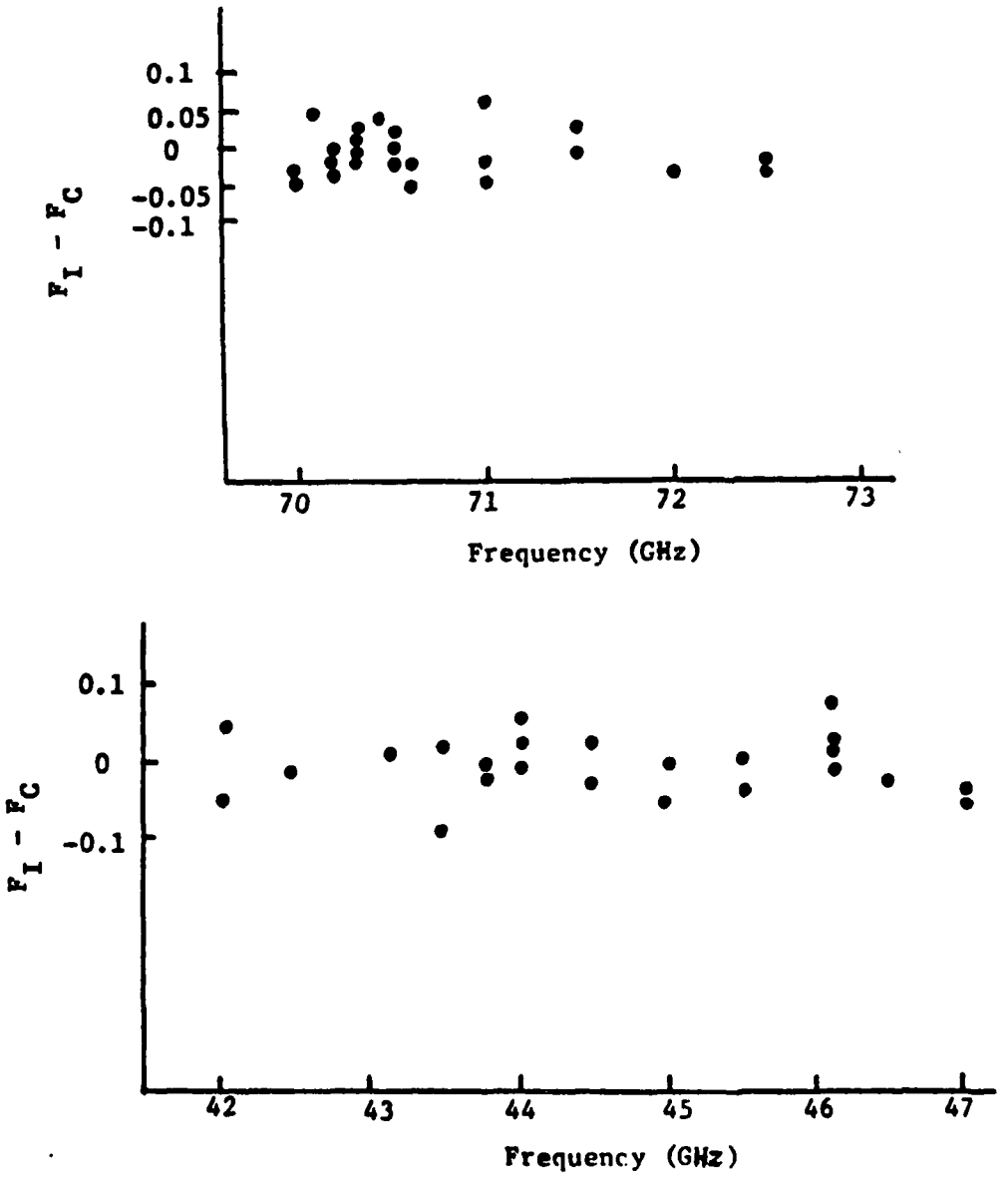

Figure 4. The difference in fractional induction versus irradiation frequency for temperature-sensitive mutants of lambda phage C600 (U16).

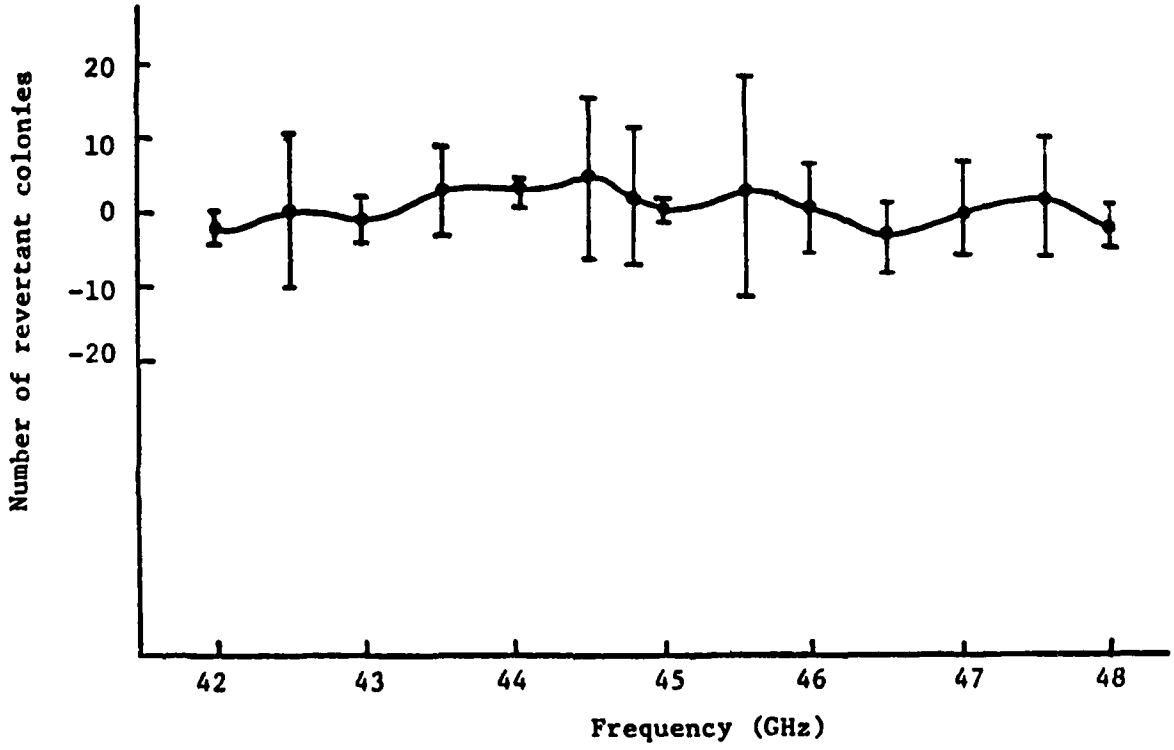

Figure 5. Number of revertant colonies versus irradiation frequency (in the U-band range) for Salmonella typhimurium cells (strain type TA1535).

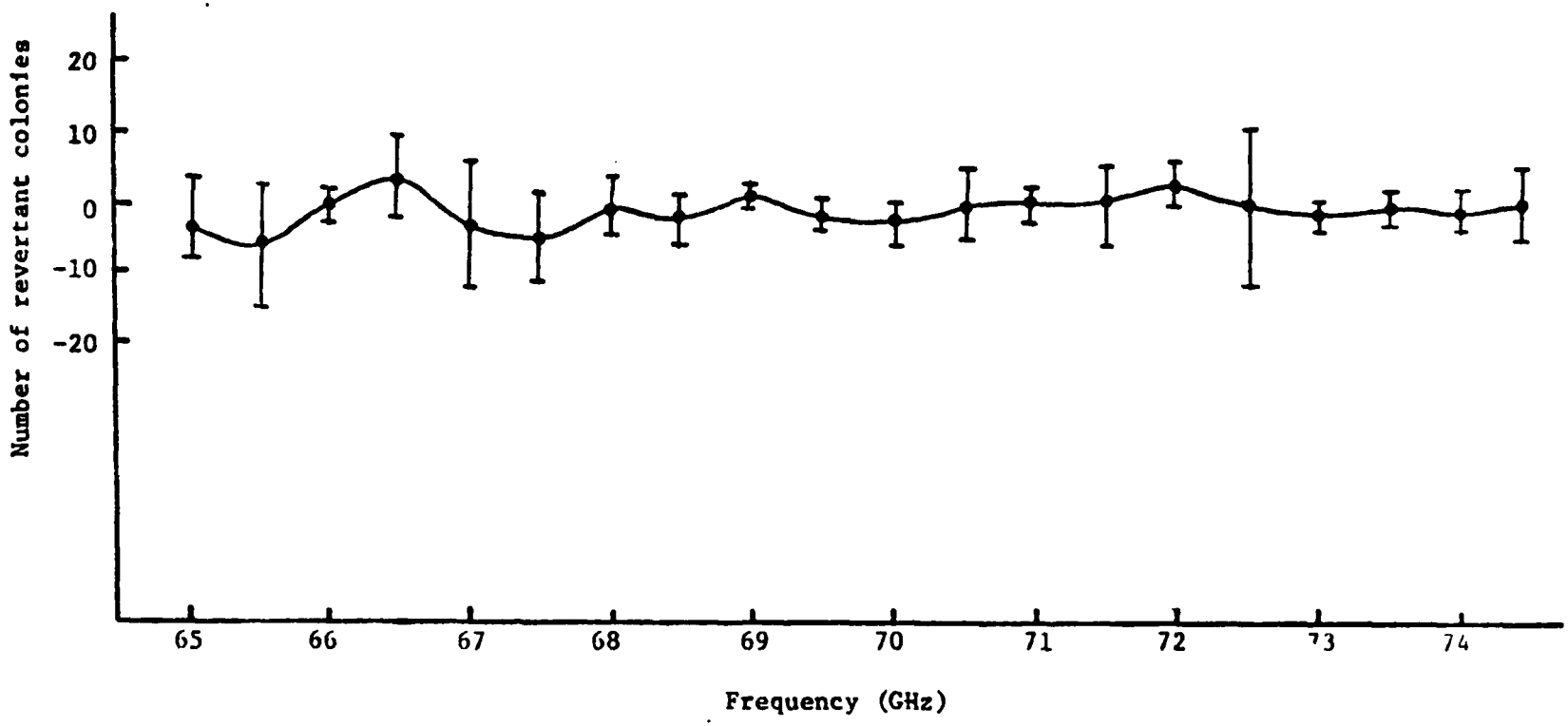

Figure 6. Results of irradiation experiments (in the E-band) using Salmonella typhimurium TA 1535 and following the Ames test procedure. The vertical bars show uncertainty due to estimated measurement error (SD).

sources (BWOs) with irradiation frequencies in the 41.5- to 41.9-GHz range stabilized to within ±1 MHz. These authors allege that these effects require irradiation frequency stability on the order of ±1 MHz. We have initiated experiments to confirm these observations. A Tektronix spectrum analyzer (model 491) was used to examine the frequency stability of our millimeter-wave klystron (OKI 40V12, 37- to 42-GHz frequency range). After a 20-minute warm-up period, its frequency variation was approximately ±3 MHz. Attempts were made to improve stability of the klystron to ±1 MHz. Variations in temperature and frequency of the klystron were monitored simultaneously to study possible contribution of temperature variations to frequency fluctuations. After the warm-up period the temperature variation of the klystron was usually within ±0.5°C and frequency fluctuation was ±3 MHz; however, there was no direct relation between temperature and sporadic frequency variations. This experiment indicated that improved cooling for the klystron will not significantly improve stability. Manual compensatory adjustment of klystron frequency was determined to be a satisfactory approach for achieving high stability for short periods (i.e., about 30 minutes). We are now evaluating electronic means of stabilizing the klystron so that a ±1-MHz stability can be maintained over periods of several hours for studying millimeter-wave effects on yeast.

Another requirement for these experiments is that frequencies in the 41.5- to 41.9-GHz band be used. Toward this end, the absolute accuracy of several frequency meters was investigated. A U-band (40-60 GHz) frequency meter (Hughes 44552H) and two Ka-band (26.5-40 GHz) frequency meters (FXR U4010A, Hughes 44550H) were connected in series and incorporated into a Ka-band irradiation setup. A Tektronix type 491 spectrum analyzer (frequency range: 10-40 GHz) was also connected to the system. A comparison of the several readings of the two Ka-band frequency meters and the spectrum analyzer verified that the two frequency meters were within 30 MHz of each other.

At frequencies near 40 GHz, the readings of the three frequency meters indicated that the U-band frequency meter is off from the Ka-band frequency meters by approximately 150 MHz. Consequently a frequency range of at least 100-150 MHz must be covered to search for the narrow-band frequency effects reported by Grundler and Keilmann [16].

PRECISION MEASUREMENTS OF THE COMPLEX PERMITTIVITIES OF BIOLOGICAL TISSUES

Theoretical and experimental investigations of a modified "infinite" sample method to obtain the complex permittivities of biological material have been carried out. The following is a summary of the work done.

Theoretical Investigations

A computer program for an infinite lossy slab in a rectangular waveguide was initially developed. In all cases studied so far, water has been considered as the test material. In the "forward problem," the complex dielectric constant, ϵ^*, of water was calculated using the Debye equations. The variation of the magnitude, $|\rho|$, and phase, ϕ, of the complex reflection coefficient, ρ^*, was studied over the frequency range 40-45 GHz. A separate computer program for the "reverse problem" (i.e., to obtain ϵ^* from a knowledge of ρ^*) has also been developed. For the case of the infinite lossy slab in the waveguide, $|\rho|$ and ϕ show only a slight variation over the frequency range considered (e.g., the case of $\epsilon_I = 1.0$ in Figures 7 and 8). Also, the values of $|\rho|$ and ϕ are such that they would involve measurements of very high voltage standing-wave ratios (VSWR) and of extremely small shifts in the position of the minimum with respect to a short termination. To overcome this problem, an intermediate lossless layer of dielectric constant ϵ_I was introduced which would act as an impedance transformer and give values of the complex reflection coefficient that vary significantly from the $1\angle 180^\circ$ value obtained when a short circuit terminates the waveguide section. A computer program has been developed to study the effect of the intermediate layer at various frequencies. To check the validity of the procedure, we decided that the measurements, in the first instance, would be made by conducting experiments in the X-band. Computed results therefore have also been obtained for the frequency range 8.2-12.4 GHz. The number of minima and the sharpness of the minima in $|\rho|$ were examined over the frequency range as a function of the length and dielectric constant of the intermediate layer. Steep variations were observed in $|\rho|$ and ϕ as a function of

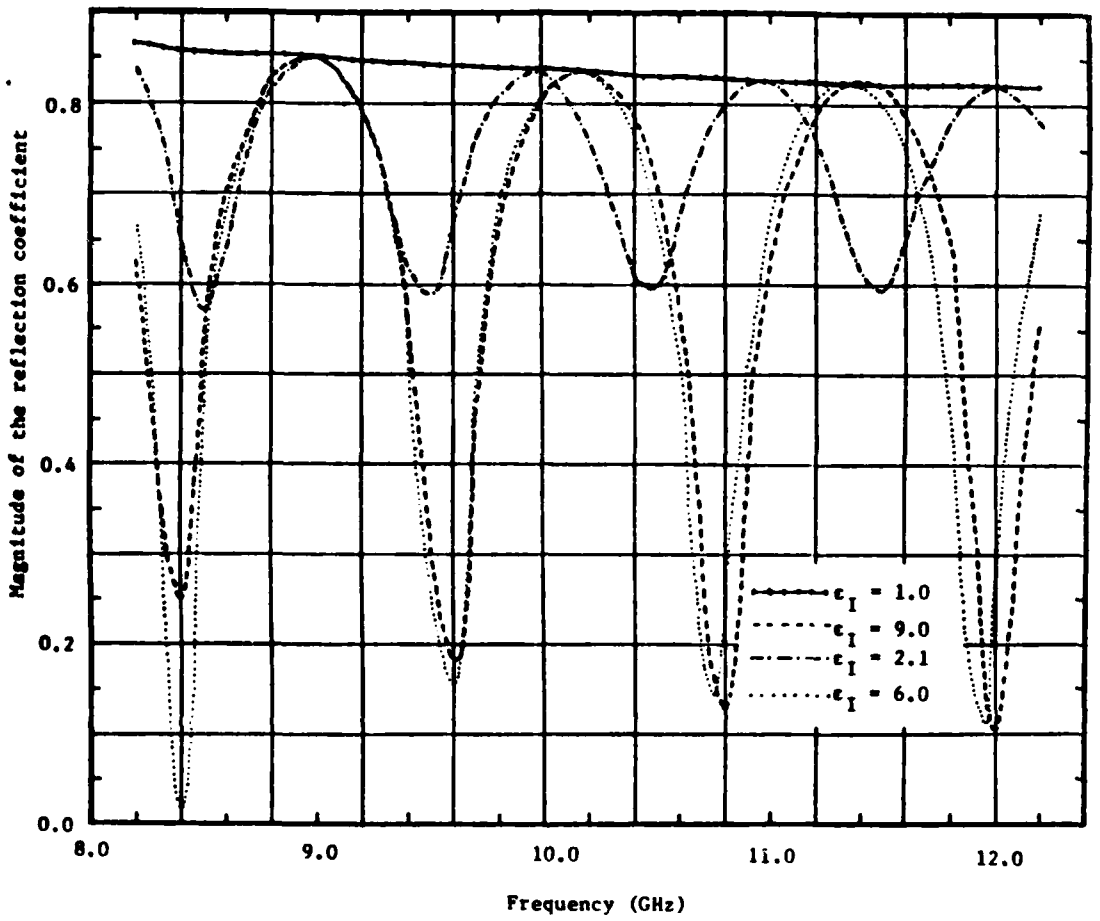

Figure 7. Variation of the magnitude of the reflection coefficient $|\rho|$ with frequency for different values of the dielectric constant ϵ_I of the intermediate layer. (Note the high, relatively invariant $|\rho|$ for ϵ_I = 1.0; i.e., without the use of an intermediate dielectric layer.)

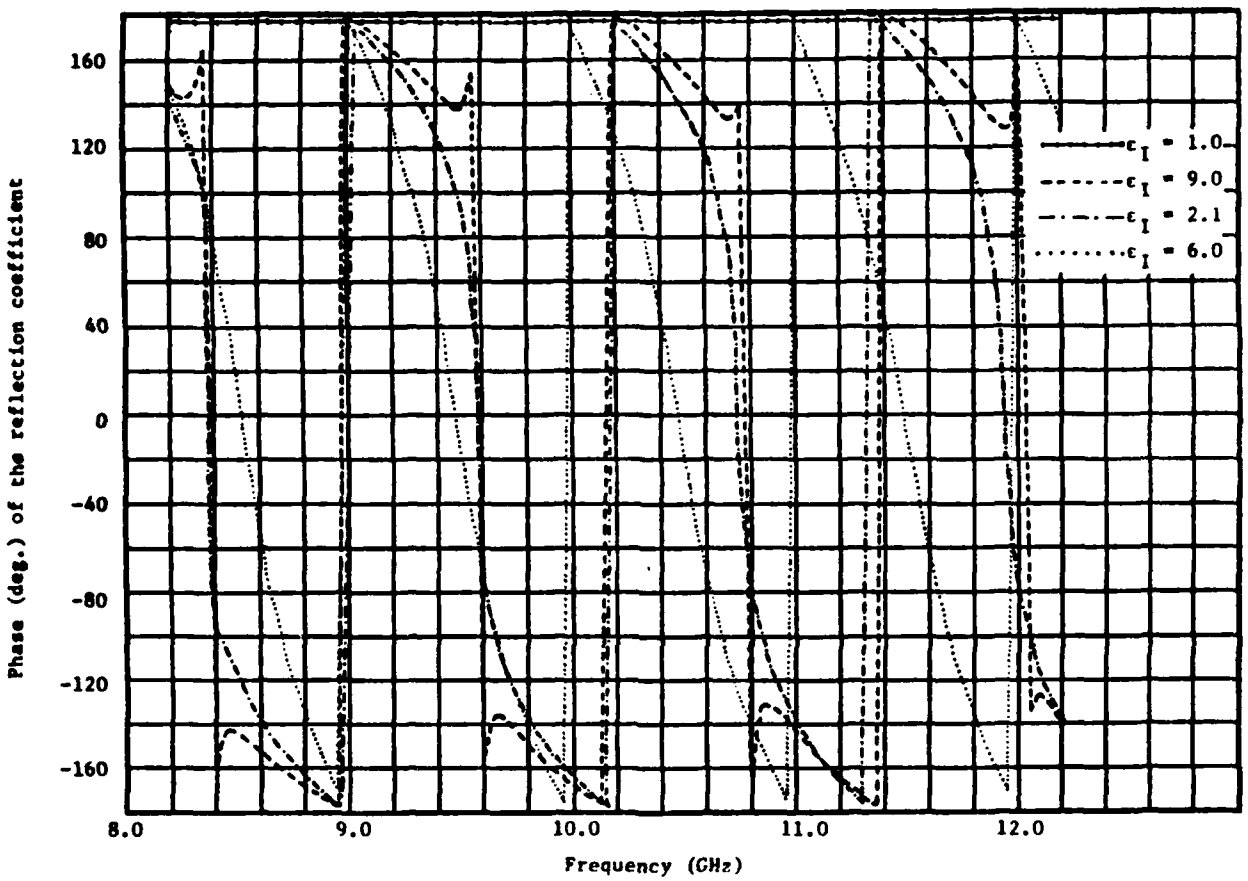

Figure 8. Variation of the phase ϕ of the reflection coefficient with frequency for different values of the dielectric constant ϵ_I of the intermediate layer. (Note the relatively invariant ϕ for $\epsilon_I = 1.0$.)

frequency; therefore, a relatively stable frequency source was required for accurate measurements. To reduce this problem somewhat, we chose a lower length equal to 3.5 guide wavelengths (at 9 GHz) for the intermediate layer; the calculations for $|\rho|$ and ϕ with frequency for this case are shown in Figures 7 and 8 for values of the dielectric constant of the intermediate layer equal to 9.0, 6.0, 2.1, and 1.0.

Errors that can be tolerated in the measurement of $|\rho|$ and ϕ at frequencies corresponding to minimum $|\rho|$ have been estimated. The calculated results are shown in Tables 1 and 2, respectively, for errors introduced in $|\rho|$ and ϕ. Errors on the order of ± 0.1 mm in the position of minimum, i.e. ϕ, and $\pm 5\%$ in $|\rho|$ can be tolerated without drastic degradation in values of ε^*.

TABLE 1. EFFECT OF ERROR IN $|\rho|$ ON THE COMPLEX PERMITTIVITY VALUES

Frequency = 8.525 GHz

Dielectric constant of the intermediate layer,

$\varepsilon_I = 2.1$

Length of the intermediate layer, L = 9.307 cm

$\|\rho\|$	Percentage Error in $\|\rho\|$	ε^*
0.5971	5	77.75 - j32.29
0.5914	4	75.44 - j30.64
0.5858	3	73.20 - j29.09
0.5801	2	71.04 - j27.63
0.5734	1	68.97 - j26.25
0.5687	0	66.96 - j24.94
0.5630	-1	65.02 - j23.71
0.5573	-2	63.15 - j22.54
0.5516	-3	61.34 - j21.44
0.5459	-4	59.59 - j20.39
0.5403	-5	57.90 - j19.41

TABLE 2. EFFECT OF ERROR IN ϕ ON THE COMPLEX PERMITTIVITY VALUES

Frequency = 8.525 GHz

Dielectric constant of the intermediate layer, $\varepsilon_I = 2.1$

Length of the intermediate layer, L = 9.307 cm

ϕ Degrees	Error in Degrees	ε^*
-1.81	5	73.99 - j52.00
-2.81	4	73.30 - j94.49
-3.81	3	72.23 - j13.59
-4.81	2	70.80 - j17.58
-5.81	1	69.03 - j21.37
-6.81	0	66.96 - j24.94
-7.81	-1	64.62 - j28.25
-8.81	-2	62.05 - j31.28
-9.81	-3	59.28 - j34.02
-10.81	-4	56.36 - j36.44
-11.81	-5	53.33 - j38.56

Experimental Investigations

The modified "infinite" sample method was used in experiments to determine the complex permittivity in the X-band. This frequency range was chosen as an initial step to check the experimental procedure and also to identify critical parameters that would affect the accuracy of measurements.

Two sets of experiments at the X-band were conducted before using the proposed infinite sample method. The first set corresponds to the measurement of the dielectric constant of Teflon. Von Hippel's procedure, which involves termination of a finite section of waveguide filled with

Teflon with a short circuit, was adopted. An 8-inch waveguide section filled with Teflon was used. Values of ε between 2.098 and 1.902 in the frequency range 9.0-10.5 GHz were obtained. These experiments indicated reasonable accuracy and consistency of the X-band equipment.

The second set of experiments used the standard infinite sample procedure for high-loss liquids to measure the complex permittivity of water. The sample holder was an open-ended waveguide section, and the end connected to the slotted section was covered by a thin mica window to ensure proper level of water in the waveguide. These experiments indicated the need for a precise procedure to measure the following:

a. Shift in the position of the minimum with respect to a short termination.

b. Accurate measurement of the high VSWR.

c. Exact leveling of water, with care to avoid air gaps.

To help reduce these problems, the experimental setup was modified such that the slotted section and the sample holder were mounted on a slow-motion drive so that the whole setup could be raised or lowered for exact adjustment of the water level. Furthermore, the slotted section was fitted with a micrometer to allow accurate measurements of the shifts in the position of the minimum with respect to a short termination.

With the experimental setup thus refined, efforts were focused on modifying the infinite sample method of measurements so as to avoid measuring very large VSWR values as well as very small shifts in minima between the sample and the short-circuit termination of the slotted section. The modified infinite sample method, which involves inserting an intermediate section of waveguide filled with an intermediate value of the dielectric constant, was adequate for minimizing the limitations of the standard infinite sample method.

The experimental setup of our proposed modified infinite sample method consists of a slotted section connected to a Teflon-filled waveguide section terminating with another waveguide section immersed in a container of water. The material Teflon was chosen due to its easy availability. The experimental procedure consists of measuring the VSWR and the shift in the position of the minimum with respect to a short termination. These give a value of the complex reflection coefficient from

which the complex permittivity can be determined with the computer program developed.

The sources of error that lead to inaccuracies in the measured values lie in the exact determination of the frequency and of the length of the intermediate dielectric layer. Errors also arise in measuring the high VSWR and determining the exact shift in the minima. Care has to be taken to avoid an air gap at the Teflon-water interface. A further step to reduce the errors is to recognize, from Figures 7 and 8, that $|\rho|$ and $|\phi|$ increase monotomically for frequencies below those for minima of VSWR. This property has been utilized to fit polynomials through the experimental data for $|\rho|$ and ϕ, as illustrated in Table 3. The polynomials so obtained are used to calculate the ϵ^* for various close-spaced frequencies over the experimental band. This is shown in Table 4 for the frequency band 8.35-8.55 GHz. At this stage, one should be able to fit a single- or double-relaxation Debye equation through the data.

TABLE 3. EXPERIMENTAL VALUES OF $|\rho|$ AND ϕ AND THE CORRECTED VALUES AFTER A POLYNOMIAL FIT THROUGH DATA WITH LEAST-SQUARE APPROXIMATION

Frequency GHz	$\lvert\rho\rvert$ Measured	$\lvert\rho\rvert$ Polynomial	ϕ Measured	ϕ Polynomial
8.335	0.733	0.734	107.13	107.77
8.360	0.707	0.708	100.97	99.27
8.385	0.682	0.678	88.36	88.20
8.410	0.647	0.648	73.73	74.69
8.435	0.620	0.619	57.69	58.99
8.460	0.595	0.594	39.63	41.46
8.485	0.572	0.577	25.70	22.55
8.510	0.566	0.568	5.31	2.82
8.535	0.572	0.569	-18.89	-17.04
8.560	0.584	0.582	-37.69	-36.27

For the present calculations, a single-relaxation Debye equation is fitted through the data for ε^* in the fourth column of Table 4; also, $\varepsilon_\infty = 5.0$ is assumed as given by several authors, e.g. Schwan and Foster [17], Cook [19]. The values of the low frequency or static dielectric constant ε_s and the relaxation time τ so calculated are given in the last

TABLE 4. VALUES OF THE PARAMETERS ε_s AND τ OBTAINED FROM EXPERIMENTAL VALUES OF ε^* ($\varepsilon_\infty = 5.0$) [8]

Frequency GHz	$\lvert\rho\rvert$ Polynomial	ϕ Polynomial	ε^*	ε_s	τ Units of 10^{-12}s
8.35	0.719	102.99	58.48 - j24.76	69.94	8.82
8.36	0.708	99.27	60.15 - j21.62	68.63	7.46
8.37	0.697	95.15	61.14 - j19.69	68.28	6.64
8.38	0.685	90.62	61.72 - j18.86	68.01	6.33
8.39	0.672	85.69	62.09 - j18.98	68.16	6.29
8.40	0.659	80.38	62.41 - j19.72	69.18	6.51
8.41	0.648	74.69	62.65 - j20.96	70.27	6.88
8.42	0.636	68.66	62.92 - j22.43	72.31	7.56
8.43	0.624	62.29	63.14 - j24.05	73.09	7.81
8.44	0.613	55.63	63.34 - j25.58	74.56	8.27
8.45	0.603	48.67	63.47 - j27.09	76.01	8.72
8.46	0.594	41.46	63.56 - j28.41	77.34	9.13
8.47	0.586	34.03	63.55 - j29.49	78.40	9.46
8.48	0.579	26.42	63.48 - j30.34	79.22	9.74
8.49	0.574	18.65	63.27 - j30.99	79.75	9.97
8.50	0.570	10.77	62.83 - j31.40	79.88	10.17
8.51	0.568	2.82	62.21 - j31.66	79.73	10.35
8.52	0.568	- 5.15	61.44 - j31.87	79.44	10.55
8.53	0.568	-13.09	60.31 - j31.88	78.69	10.75
8.54	0.571	-20.97	58.98 - j31.98	77.93	11.04
8.55	0.575	-28.71	57.52 - j32.09	77.13	11.37
		Mean values:		74.57	8.75

two columns of Table 4. The average values of $\varepsilon_s = 74.57$ and $\tau = 8.75 \times 10^{-12}$ sec are in good agreement with those given by other authors [17-19] (see Table 5).

Obviating the need for precisely fabricated submillimeter-length sample holders [8, 9], this novel procedure promises to allow accurate measurements of the complex dielectric properties of the biological media over the 26.5- to 90-GHz band for whch the solid-state computer-controlled precision measurement facilities are currently available in our laboratory [10]. With slight modifications, the method developed here may also lend itself to measurements of the tissues in vivo.

TABLE 5. PRESENT-EXPERIMENT VALUES OF ε_s, ε_∞, AND τ FOR WATER COMPARED TO VALUES GIVEN BY OTHER AUTHORS

	ε_s	ε_∞	τ Units of 10^{-12} s
Present method	74.57	5.0	8.75
Schwan and Foster [17]	77.0	4.9	7.50
Collie, Hasted, and Ritson [18]	80.36	5.5	9.55
Cook [19]	81.0	5.0	9.0

LASER BRILLOUIN AND RAMAN SPECTROSCOPY OF BIOLOGICAL SYSTEMS

To estimate the lowest frequency vibrational mode of cell membrane, we initiated a theoretical modeling of membrane. In our model the hydrophilic part of the phospholipid is considered as a rigid mass and the hydrophobic carbon chain as a series of springs. The model is illustrated by Figure 9. From Figure 9b, the effective-force constant is given by:

$$K_{eff} = \left[K_1^{-1} + K_2^{-1} + \ldots + K_{17}^{-1} + K_{18}^{-1}\right]^{-1} + \left[(K_1')^{-1} + (K_2')^{-1} + \ldots + (K_{17}')^{-1} + (K_{18}')^{-1}\right]^{-1} = \frac{1}{9} K.$$

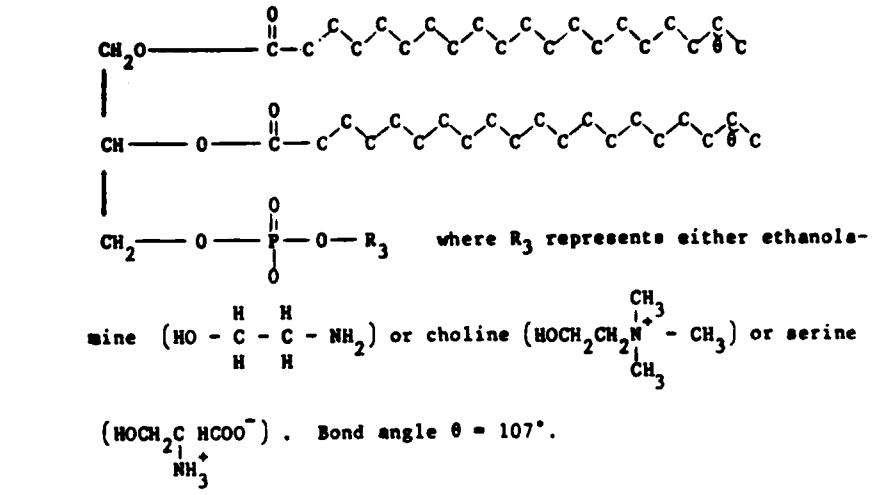

(a)

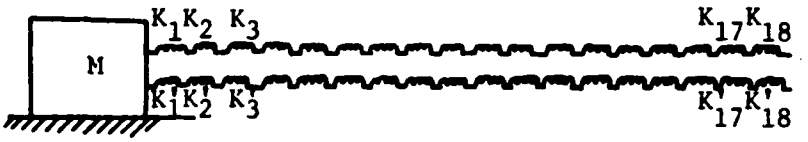

(b)

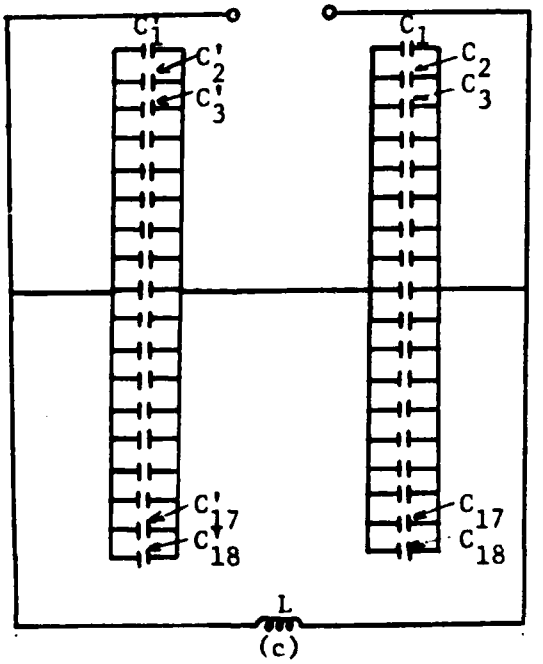

(c)

Figure 9. Model of a cell membrane. (a) The phospholipid, (b) the equivalent mechanical model, and (c) the equivalent electrical circuit which is obtained from the mechanical model via analogy M → L and K → 1/C.

The spring-force constant K is related to the force constant for C-C bond K':

$$K = K' \cos \left[\frac{1}{2}(180 - 107)\right].$$

The mass of the hydrophilic component M may be expressed in terms of its components:

$$M = 7\,M_C + 8\,M_O + 11\,M_H + M_P + M_N$$

where we have assigned ethanolamine (i.e., $HO - \overset{H}{\underset{H}{C}} - \overset{H}{\underset{H}{C}} - NH_2$) to R_3; M is the mass in atomic units; and subscripts C, O, H, P, and N represent carbon, hydrogen, phosphorous, and nitrogen respectively. Consequently, M = 268.139 amu = 4.452×10^{-25} kg. Using the value [20] of 3.1 mdyn/Å (≡ 310 N/m) for K', the frequency of vibration is:

$$f = \frac{1}{2\pi}\left(\frac{K_{eff}}{M}\right)^{1/2} = 1.255 \times 10^{12}\,\text{Hz} \equiv 41.861\ \text{cm}^{-1}.$$

A detailed experimental study of vibrational modes of liposomes will be performed (via Raman scattering), and the results will be compared with the theoretical value.

Systems were designed and tested for Brillouin and Raman studies of biological entities. The Brillouin setup is shown in Figure 10. The beam from an argon ion laser (Spectra Physics 165) is focused on the center of a sample holder (a glass tubing of rectangular cross sections). Lens L_2 forms an image of the scattered light on the entrance slit of a double spectrometer (Spex 1403). The light that emerges out of the spectrometer is focused on the entrance mirror of a Fabry-Perot interferometer (FPI, RC-40) which is operated in scanning mode to assure passage of the illuminating frequency. The output beam from the FPI reaches the PM tube (EMI 9558A) through a small pinhole. Photon accumulation and processing is achieved by means of an amplifier discriminator (Ortec 9302) and a data acquisition/utilization network (Burleigh DAS-1). DAS-1 also serves the function of scanning and maintaining the FPI at optimum alignment over

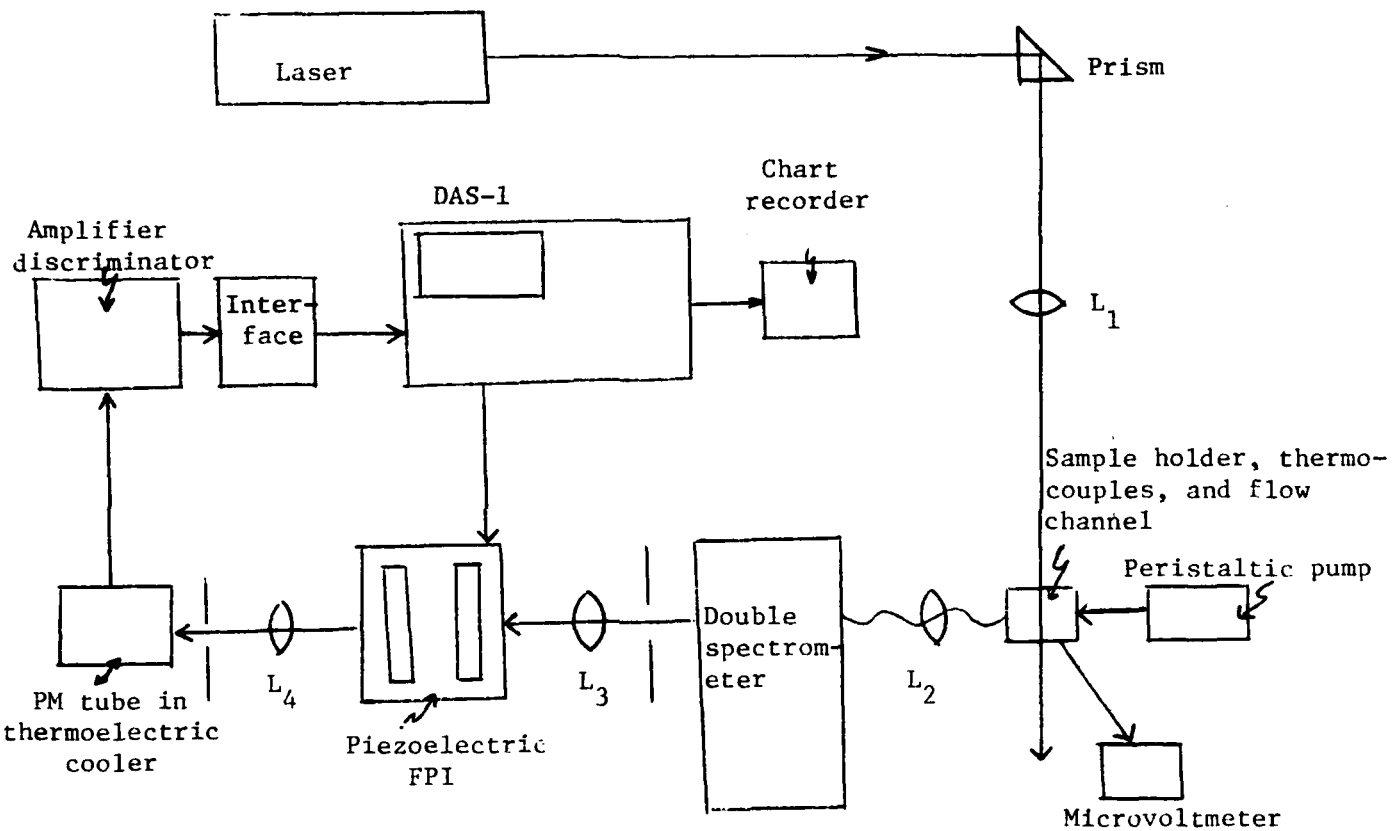

Figure 10. Block diagram of Brillouin spectroscopy system.

long periods. The spectra are recorded by means of a stripchart recorder (Soltec VP62325).

In Brillouin spectroscopy, minimizing the laser linewidth is important; therefore, an etalon is placed inside the laser cavity. A temperature regulatory system, consisting of a peristaltic pump (which circulates the aqueous samples) and a thermally controlled water bath, is used to minimize the sample heating by the laser beam. A series of copper-constantan thermocouples and a microvoltmeter (Keithly Instruments 150A) are also incorporated into the system to allow measurement of temperature differences between the ports of the sample holder and the water bath. Some significant characteristics of this system include:

a. Excellent resolution of ≈ 0.15 cm^{-1}.

b. High contrast, as the FPI can be operated in multipass mode. (Contrast for single-pass operation is 340 as compared to a contrast of 3.9×10^7 for three-pass and 4.5×10^{12} for five-pass, when mirror reflectivity is 90%.)

c. Provision for investigating weak spectra, which may require signal integration over a period of several hours.

d. Control and monitoring of sample temperature.

e. Provision for providing oxygen to the biological cells.

In collaboration with Dr. Laura Kingsford, Department of Microbiology, California State University, Long Beach, California, efforts have been initiated to prepare for the necessary experiments on the laser Raman spectrographic analysis of liposomes and related structures. As part of the proposed ongoing research, suspensions of liposomes prepared by sonication of mixtures of phosphatidylcholine and water [21] have been studied. This method, based upon differential centrifugation, yields preparations reported to be of equivalent-size homogeneity to those obtained by molecular-sieve chromatography.

Specific viral glycoproteins G1 and G2 from LaCrosse virus have been prepared, labeled with ^{35}S-methionine [22], and will be used to make virosomes composed of phospholipid bilayer vesicles (liposomes) with inserted virus glycoprotein (virosome). Investigation of these structures with one higher order of complexity toward a cytoplasmic membrane by laser Raman spectroscopy is planned for the future.

Figure 11 illustrates our setup for Raman spectroscopy, which is quite similar to the Brillouin setup. The main difference is that the Fabry-Perot interferometer has been removed. The system allows investigation of spectra over a wide frequency range (3 cm^{-1} to 4000 cm^{-1}). The Raman and Brillouin spectroscopy systems have been tested and a series of experiments has been carried out, including:

a. Brillouin spectroscopy of carbon tetrachloride (Brillouin shift was obtained around 7-9 GHz for laser wavelength of 4880 Å and 90° scattering).

b. Raman spectroscopy of 1, 2, 4 trichlorabenzene (a line was observed at $\Delta f \approx 468$ cm^{-1}).

c. Raman spectroscopy of water under flowing conditions.

d. Raman and Brillouin spectroscopy of biological media such as phosphate-buffered saline (PBS), PBS without Ca^{++} and Mg^{++} (PD), and M-9 modified (containing salts and ammonia sulfate, and supplemented with essential amino acids).

e. Spectral scan of E. coli suspension in PBS (for an FPI free spectral range of 15 GHz), which is shown in Figure 12. The spectra indicate that Brillouin shift for E. coli suspension is 5.6 GHz.

f. An interferometric scan of E. coli in M-9 (modified) with FPI free spectral range set at 100 GHz. A large integration time of 68 minutes was used. The result, which is presented in Figure 13, verifies that the only structure in the 0-100 GHz range is the Brillouin peak. (The Brillouin line at 5.6 GHz can be seen clearly when the free spectral range of the FPI is set at 15 GHz, as illustrated by Figure 12.)

g. Raman scan of E. coli in PD + $(NH_4^+$-glucose) in the range 15 cm^{-1} to 330 cm^{-1}, which is presented in Figure 14. The result suggests that no spectra are present, contrary to reports by other investigators [23].

h. A computer program was written to multiply the Raman scan by $(1 - e^{-h\Delta f/kT})$, where Δf is the frequency shift from the laser line; h the Planck's constant; k the Boltzmann's

constant, and T the temperature of the sample. As illustrated in Figure 15 for the PBS solution, this helps to mask out the unwanted Rayleigh scattering (e.g., Figures 12 and 13) that is so typical of the Raman scans. The system is now poised to undertake studies on low-wave-number Raman spectroscopy of biological media.

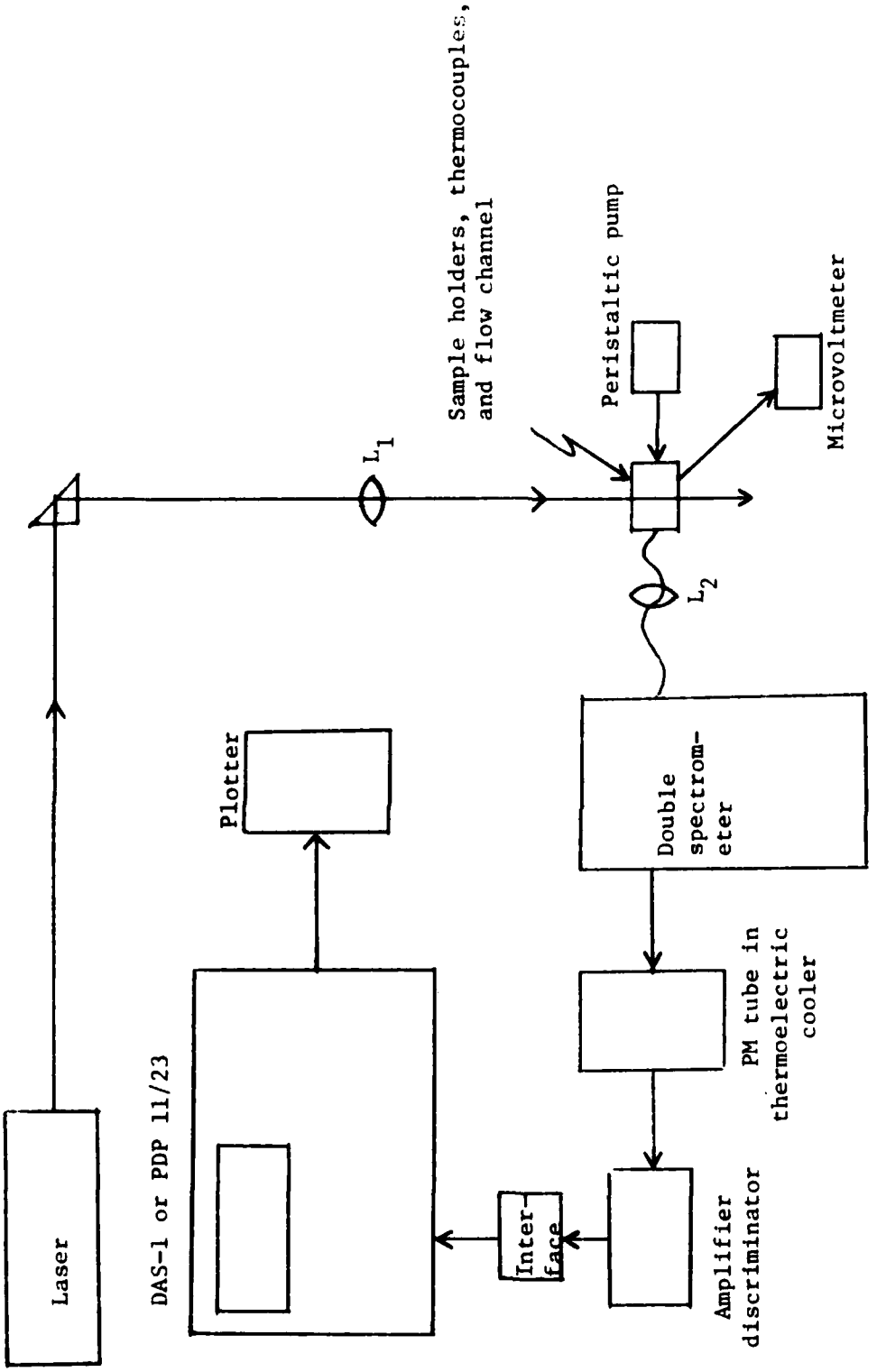

Figure 11. Setup for Raman spectroscopy.

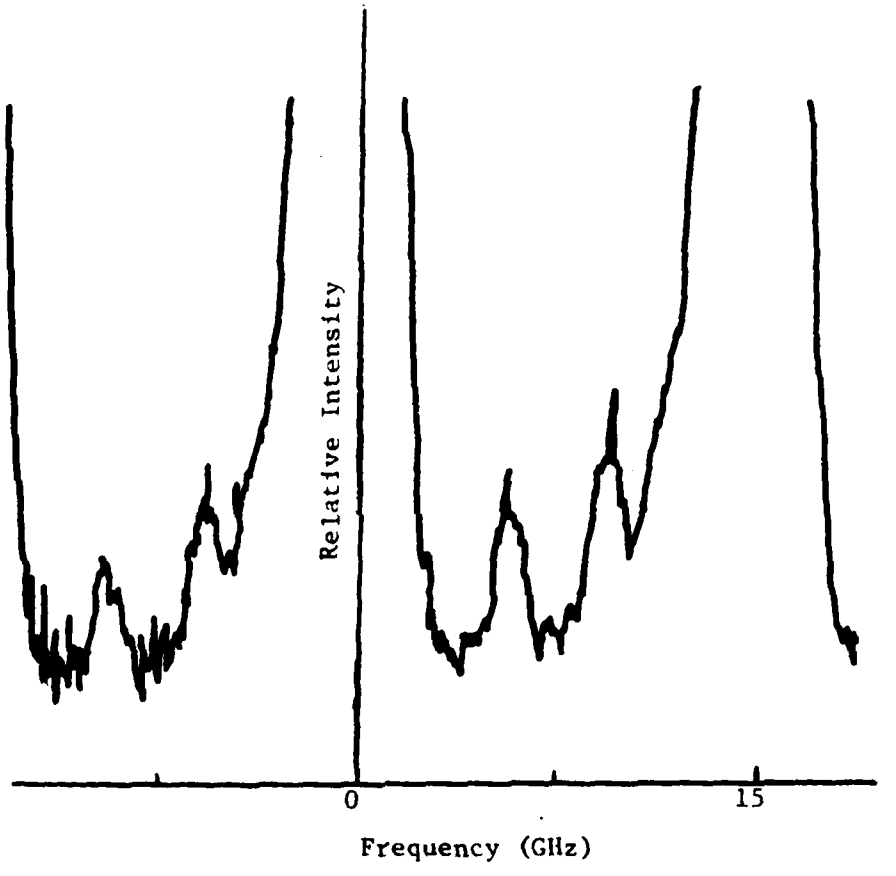

Figure 12. Brillouin spectra of E. coli suspensions in PBS when free spectral range of FPI is 15 GHz.

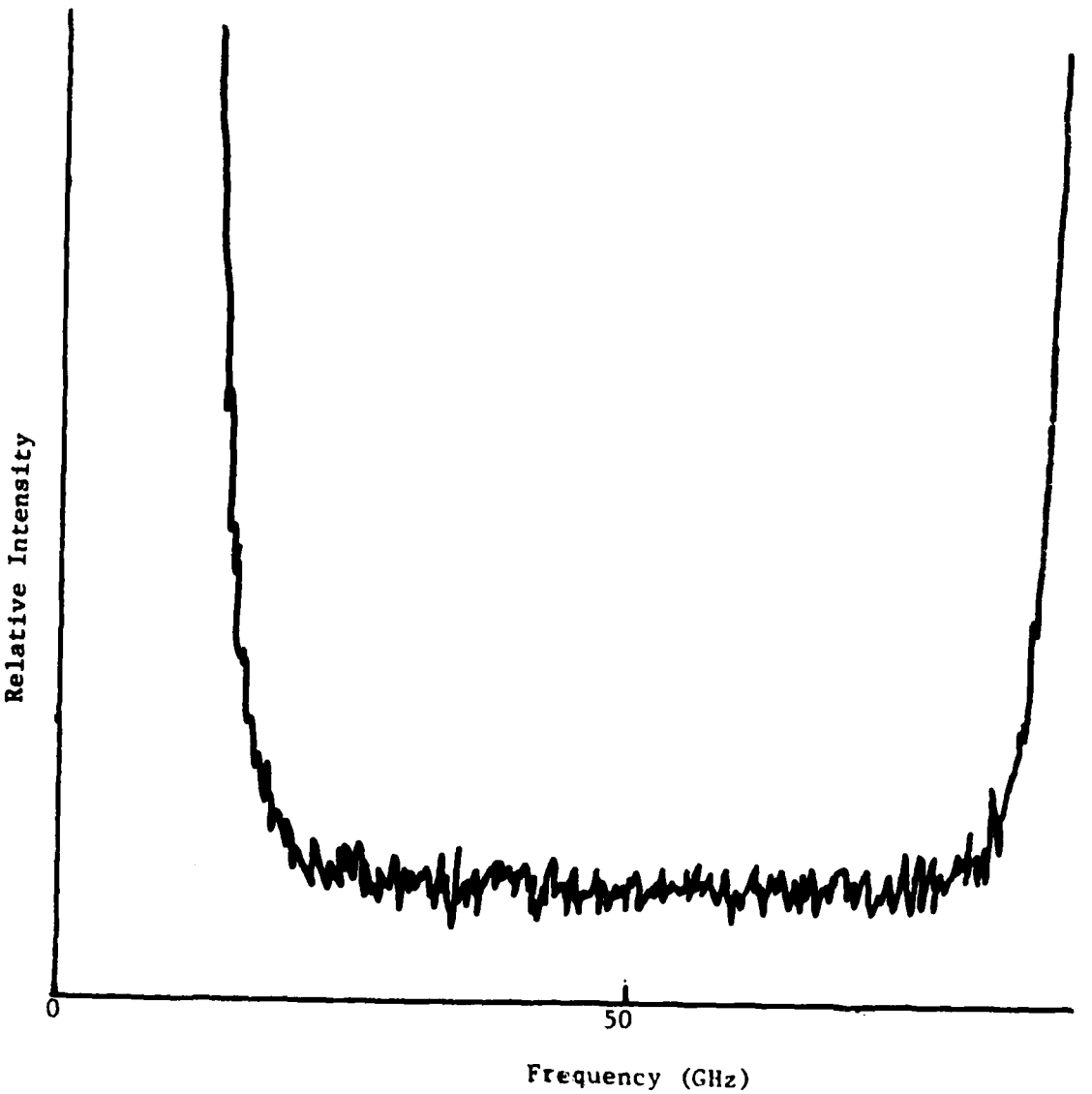

Figure 13. Interferometric scan of E. coli suspension in M-9 (modified) with free spectral range of FPI set at 100 GHz.

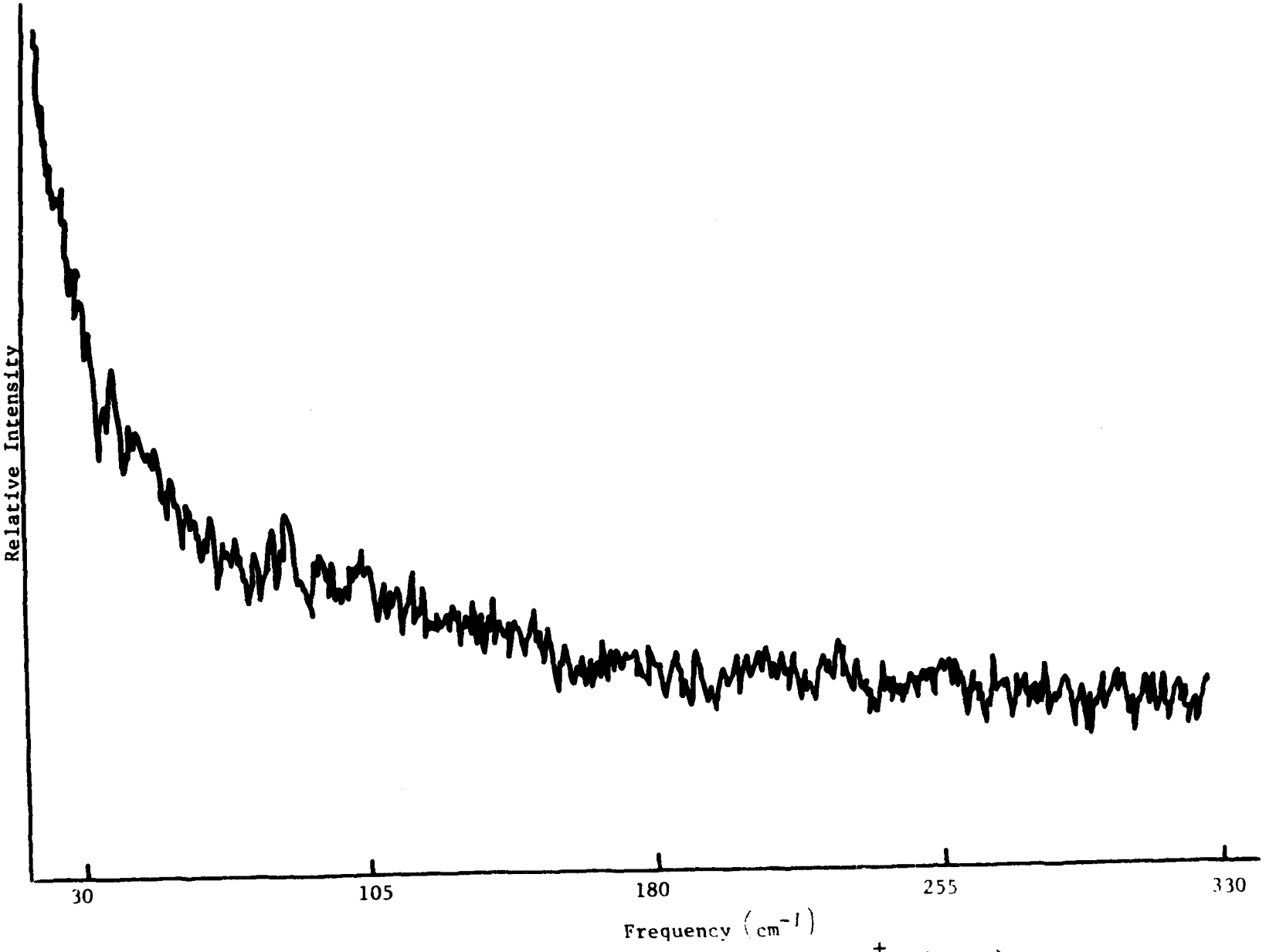

Figure 14. Raman scan of E. coli in PD + (NH_4^+ -glucose).

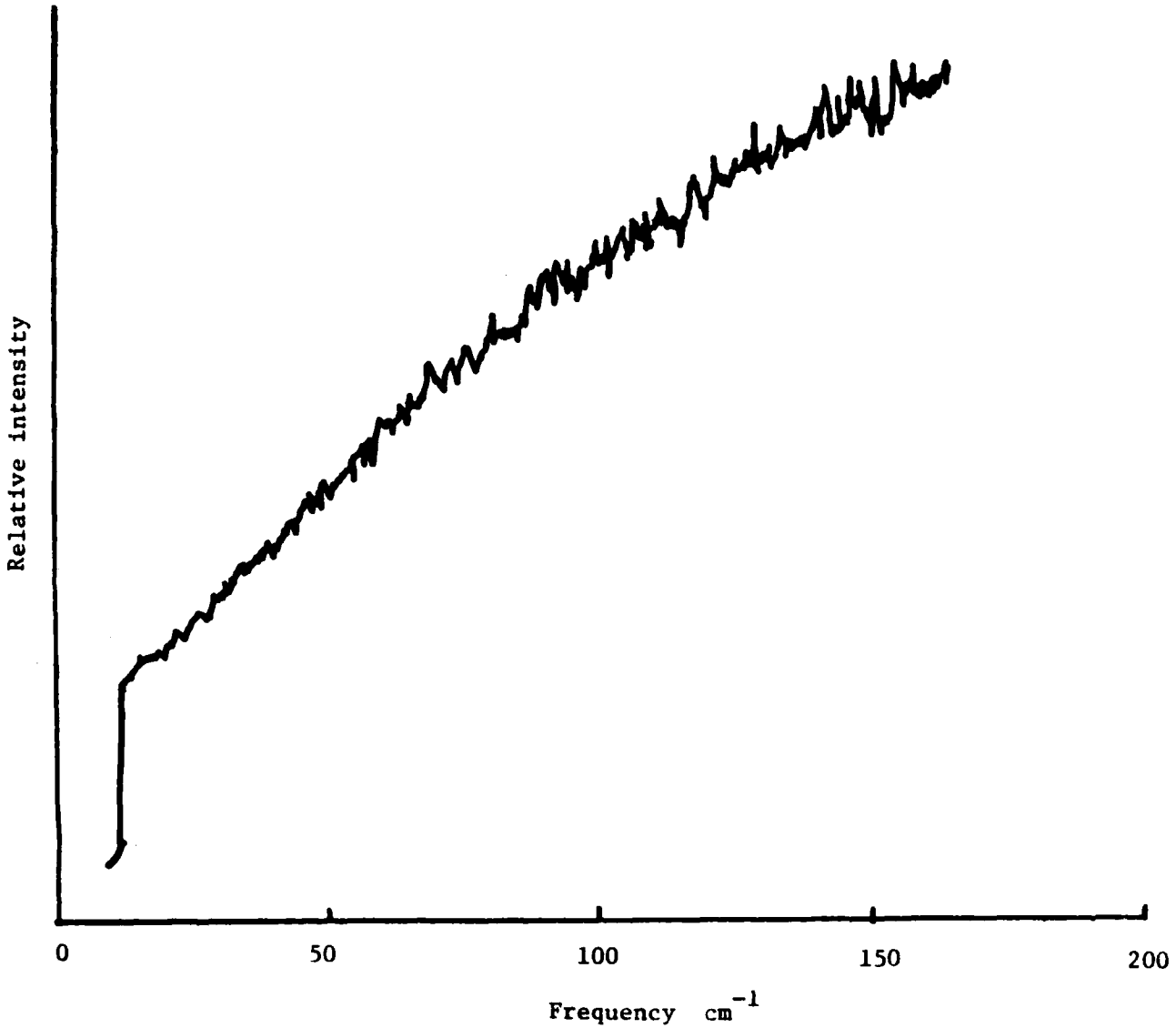

Figure 15. The result of multiplying the intensity of the Raman scan of PBS by the factor ($-h\Delta f/kT$).

REFERENCES

1. Devyatkov, N. D., et al. Highlights of the papers presented on millimeter wave biological effects. Sov Phys--Usp 4:568-579 (1974).

2. Berteaud, A. J., et al. Action d'un Rayonnement electromagnetique a'longuer d'onde millimetrique sur la croissance Bacterienne. Comptes Rendus Acad Sci (Paris) 281:843-846 (1975).

3. Sevastianova, L. A., and S. L. Potopov. Resonance effect in biological action of microwave radiation. Paper presented at 1976 URSI meeting, Amherst, Massachusetts.

4. Grundler, W. Recent results of experiments on nonthermal effects of millimeter microwaves on yeast growth. Coll Phenom 3:181-186 (1981).

5. Partlow, L. M., et al. A novel in vitro method for study of thermal and athermal bioeffects of microwave irradiation on monolayer cultures. Bioelectromagnetics 2:123-140 (1981).

6. Stensaas, L. J., et al. Thermal and athermal bioeffects of microwave irradiation on monolayer cultures of BHK-21/C13 cells assessed by scanning and transmission electron microscopy. Bioelectromagnetics 2:141-150 (1981).

7. Bush, L. G., et al. Effects of millimeter-wave radiation on monolayer cell cultures. III. A search for frequency-specific athermal biological effects on protein synthesis. Bioelectromagnetics 2(2): 151-159 (1981).

8. Szwarnowski, S., and R. J. Sheppard. Precision waveguide cells for the measurement of permittivity of lossy liquids at 70 GHz. J Phys 10E:1163-1167 (1977).

9. Van Loon, R., and R. Finsy. The precise microwave measurements of liquids using a multipoint technique and curve-fitting procedure. J Phys 8D:1232-1243 (1975).

10. Gandhi, O. P., et al. Millimeter wave absorption spectra of biological samples. Bioelectromagnetics 1:285-298 (1980).

11. Jacobson, A. G., and Y. R. Shen. Coherent Brillouin spectroscopy. Appl Phys Lett 34:464-467 (1974).

12. Wang, C. H., et al. Brillouin scattering and segmental motion of a polymeric liquid, II. Mol Phys 37:287-298 (1979).

13. Fröhlich, H. Coherent electric vibrations in biological systems and the cancer problem. IEEE Trans Microwave Theory Tech MTT-26: 613-617 (1978).

14. Riazi, A., et al. A broadband temperature-controlled system for the study of cellular bioeffects of microwaves. IEEE Trans Microwave Theory Tech MTT-30:1996-1998 (1982).

15. Webb, S. J. Factors affecting the induction of lambda prophages by millimeter microwaves. Phys Lett 73A:145-148 (1979).

16. Grundler, W., and F. Keilmann. Nonthermal effects of microwaves on yeast growth. Z Naturforsch 33C (1/2):15-22 (1978).

17. Schwan, H. P., and K. R. Foster. RF-field interactions with biological systems: Electrical properties and biophysical mechanisms. Proc IEEE 68:104-113 (1980).

18. Collie, C. H., et al. The dielectric properties of water and heavy water. Proc Phys Soc London 60:145-160 (1948).

19. Cook, H. F. A comparison of the dielectric behavior of RF pure water and human blood at microwave frequencies. Br J Appl Phys 3:249-255 (1952).

20. Fanconi, B., et al. Phonon dispersion curves and normal coordinate analysis of α-poly-L-alanine. Biopolymers 10:1277-1298 (1971).

21. Barenholz, Y., et al. A simple method for the preparation of homogeneous phospholipid vesicles. Biochemistry 16:2806-2810 (1977).

22. Kingsford, L., and D. W. Hill. The effects of proteolytic enzymes on structure and function of LaCrosse G1 and G2 glycoproteins. In D. H. L. Bishop and R. W. Compans (eds). Replication of negative strand viruses. New York: Elsevier-North Holland Pub Co., 1981.

23. Webb, S. J., and M. E. Stoneham. Resonances between 10^{11} and 10^{12} Hz in active bacterial cells as seen by Raman spectroscopy. Phys Lett 60A:267-268 (1977).

END

FILMED

9-83

DTIC